

# Analytical-Based Iron Loss Assessment in the SPM Slotless Machine Stator Core

Matteo Leandro<sup>1\*</sup>, Nada Elloumi<sup>2</sup>, Alberto Tessarolo<sup>2</sup> and Jonas Kristiansen Nøland<sup>1</sup>

<sup>1</sup> Department of Electric Power Engineering, Norwegian University of Science and Technology, Trondheim, Norway

<sup>2</sup> Engineering and Architecture Department, University of Trieste

\*E-mail: matteo.leandro@ntnu.no

**Abstract**—The use of slotless machines has acquired growing interest when features such as low vibrations and noise, along with low losses at high speed, are required. However, a careful assessment of the iron losses in the stator core will be relevant already in the design or pre-design phase. Standard methodologies for the iron losses estimation are typically FE analysis with constant coefficients (dummy model), which can lead to weak extrapolations with huge errors. In this paper, an analytical method for iron losses prediction is derived. It is based on the extension of the field solution in the stator iron core, where an accurate 2-D field solution of the slotless machine topology is found. The analytical solution is combined with a variable coefficient loss model, which can be efficiently computed by vectorized post-processing. The case study proves that the approach can predict all of the loss phenomena over a wide operating range with improved precision.

**Index Terms**—Slotless machine, analytical method, Laplace’s equation, magnetic field, stator core, iron losses, rotational losses.

## I. INTRODUCTION

Slotless machines eliminate the slotting effect and related additional losses, as well as the cogging torque. It is an attractive topology for machines operating in ultra-high speeds. As of today, different works have been dealing with analytical modeling of slotless machines [1]–[5]. The analytical field solution has been utilized to propose an iron loss estimate method based on constant coefficients [6]. Moreover, an extended method has been formulated with a two-component iron loss calculation in a soft magnetic composite stator core [3]. The finite iron permeability was also considered, as for SMC material assuming infinite iron permeability would lead to a non-negligible discrepancy with respect to a real case.

In a general instance, the iron losses evaluation can be divided into two main steps. The first step is the estimation of the flux density in the iron parts carrying a time-varying magnetic field. To this end, the generalized field solution considering different magnet patterns will be used for a general evaluation of the flux density in the stator core. The second step is to fit the post-processing of the estimated magnetic field to a suitable model defining the losses in the iron material. The latter point has been object of several other works. Time-based and frequency-based iron loss models are used interchangeably, albeit giving different results [7], [8] (with a variation within the accuracy of the outcome). Several iron loss models, based on variable loss coefficients ([9]–[11]), showed the effective achievement of a better fitting to

experimental data. A further improvement in the iron loss estimate in rotating electrical machines, may be given by the inclusion of the rotational effect; in reference [7] the rotational effect is applied to a case study. The proposed methodology implements some of the above mentioned contributions for the sake of testing its flexibility and adaptability to the most used iron loss models.

The remainder of the paper is organized as follows. Section II describes the problem formulation. Then, Section III derives the analytical formulation of the magnetic field in the stator core. The loss estimation results are presented in Section IV. Finally, Section V concludes the paper.

## II. ANALYTICAL MODEL DEFINITION AND ASSUMPTIONS

The slotless SPM has a simple 2-D geometry, composed of coaxial annular sections with smooth boundaries (Fig. 1). As a result, a very accurate and computationally efficient analytical field solution can be formulated ([4], [12], [13])

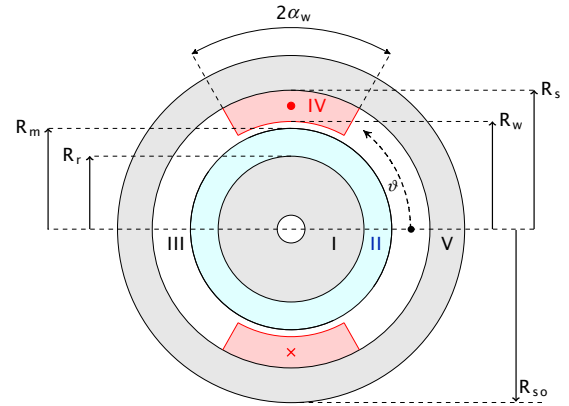


Fig. 1. Domains on a sample inrunner geometry with only one phase.

The field problem definition is based on the following fundamental assumptions (to be applied to Fig. 1):

- The 3-D end-effects are neglected, i.e., the magnetic vector potential is treated as a scalar quantity lying orthogonal to the 2-D plane in all domains;
- The magnetic permeability of rotor and stator core (regions I and V, respectively) is assumed to be infinite;
- The formulation of the field from the stator current assumes the relative permeability permanent magnets to be equal to unity;

- For any magnets pattern, in region II the magnetization distribution is defined for modeling the field from the magnets array;
- The stator winding is assumed to carry a three-phase balanced and symmetric sinusoidal current;

### III. FIELD EVALUATION IN THE STATOR CORE

In this section, the field solution in the stator iron core is described from its different contributions, i.e., the stator currents and the permanent magnets, respectively. Different magnet patterns can be considered. The field solution in the winding region from the two different sources is first described and then extended in the stator core region by means of suitable interface conditions.

#### A. 3.1 Stator Currents Contribution

In a cylindrical coordinate system  $(r, \vartheta, z)$  the formulation of the problem in the stator core region obeys to the following Laplace's equation:

$$\nabla^2 \mathbf{A} = \frac{1}{r} \frac{\partial}{\partial r} \left[ r \frac{\partial A_z}{\partial r} \right] + \frac{1}{r^2} \frac{\partial^2 A_z}{\partial \theta^2} = 0 \quad (1)$$

where  $\mathbf{A}$  is the magnetic vector potential, and  $A_z$  its only scalar component. Using the method of separation of variables along with the Fourier series expansion to account for all the harmonics introduced by the source of the field, the solution to (1) can be expressed as:

$$\begin{aligned} A_{z,J}(r, \theta_s, t) = & \\ & \sum_{k_p=5p, 11p, \dots}^{\infty} \left( V_{k_p}^+ r^{k_p} + V_{k_p}^- r^{-k_p} \right) \cos(k_p \theta_s + \omega t) \\ & + \sum_{k_m=1p, 7p, \dots}^{\infty} \left( V_{k_m}^+ r^{k_m} + V_{k_m}^- r^{-k_m} \right) \cos(k_m \theta_s - \omega t) \end{aligned} \quad (2)$$

the coefficients  $V_n^+$  and  $V_n^-$  are to be determined by enforcing boundary conditions with the field solution in the winding region at the radius  $R_s$ . The flux density of the 2-D problem can be expressed as a function of the scalar magnetic potential as it follows:

$$B_{r,J}^{st}(r, \theta_s) = \frac{1}{r} \frac{\partial A_{z,J}(r, \theta_s)}{\partial \theta_s} \quad (3)$$

$$B_{\theta,J}^{st}(r, \theta_s) = -\frac{\partial A_{z,J}(r, \theta_s)}{\partial r} \quad (4)$$

By means of the latter expressions it is possible to set the following boundary conditions, and given that they must hold for each and every harmonic component and any angular coordinate  $\vartheta$ , only two unknowns ( $V_n^+$  and  $V_n^-$ ) are to be found :

$$B_{r,J}^{st} \Big|_{r=R_{se}} = \frac{1}{r} \frac{\partial A_{z,J}}{\partial \theta_s} \Big|_{r=R_{se}} = 0 \quad (5)$$

$$\left( B_{r,J}^{st} = \frac{1}{r} \frac{\partial A_{z,J}}{\partial \theta_s} = B_{wr,J} \right) \Big|_{r=R_s} \quad (6)$$

Boundary condition (5) is nothing more than the magnetic insulation applied to the outer boundary and justified by the

infinite iron permeability assumption; whereas (6) gives the continuity of the radial flux density component on the interface between stator winding and iron core. The flux density in the winding region due to the stator currents  $B_{wr,J}$  is found and expressed as explained in [4] and reported in the following with the same notation:

$$\begin{aligned} B_{wr,J}(r, \theta_s, t) = & - \sum_{k_p=5p, 11p, \dots}^{\infty} \frac{k_p}{r} w_k(r, k_p) \cos(k_p \theta_s + \omega t) \\ & - \sum_{k_m=1p, 7p, \dots}^{\infty} \frac{k_m}{r} w_h(r, k_m) \cos(k_m \theta_s - \omega t) \end{aligned} \quad (7)$$

The two constants  $V_n^+$  and  $V_n^-$  are determined by substituting (2) in the boundary conditions (5) and (6). The solution of the linear system leads to the following expressions:

$$V_n^- = \frac{R_s^n R_{so}^{2n} \cdot w(R_s, n)}{R_s^{2n} - R_{so}^{2n}} \quad (8)$$

$$V_n^+ = \frac{R_s \cdot w(R_s, n)}{R_{so}^{2n} - R_s^{2n}} \quad (9)$$

Therefore, according to (3) and (4) the radial and circumferential component of the flux density in the stator core can be expressed as it follows:

$$\begin{aligned} B_{r,J}^{st}(\theta_s, r, t) = & \\ & - \sum_{k_p=5p, 11p, \dots}^{\infty} k_p \left( V_n^+ r^{k_p-1} + V_n^- r^{-k_p-1} \right) \sin(k_p \theta_s + \omega t) \\ & - \sum_{k_m=1p, 7p, \dots}^{\infty} k_m \left( V_n^+ r^{k_m-1} + V_n^- r^{-k_m-1} \right) \sin(k_m \theta_s - \omega t) \end{aligned} \quad (10)$$

$$\begin{aligned} B_{\theta,J}^{st}(\theta_s, r, t) = & \\ & - \sum_{k_p=5p, 11p, \dots}^{\infty} k_p \left( V_n^+ r^{k_p-1} - V_n^- r^{-k_p-1} \right) \cos(k_p \theta_s + \omega t) \\ & - \sum_{k_m=1p, 7p, \dots}^{\infty} k_m \left( V_n^+ r^{k_m-1} - V_n^- r^{-k_m-1} \right) \cos(k_m \theta_s - \omega t) \end{aligned} \quad (11)$$

#### B. Permanent Magnets Field Contribution

The magnet can be modeled by means of an equivalent current density [4], which is very effective for torque computation. However, a magnetization distribution in the region of the magnets is intuitive and a widely adopted course in the literature [14]–[17]. The magnetization distribution adopted in this paper can be expressed as a Fourier series along the radial and circumferential direction as follows:

$$M_r = \sum_{n=1p, 3p, \dots}^{\infty} M_{rn} \cos(n\vartheta_r) \quad (12)$$

$$M_{\vartheta} = \sum_{n=1p, 3p, \dots}^{\infty} M_{\vartheta n} \sin(n\vartheta_r) \quad (13)$$

where  $M_{rn}$  and  $M_{\vartheta n}$  are the resulting Fourier series coefficients given by the sum of the contributions of all the magnets belonging to the array to be studied. The implicit expression of the aforementioned contributions is reported in Appendix of [14]. Moreover, the angular coordinate  $\vartheta_r$  is here referred to the rotating coordinates system, differently from the stator current field solution where  $\vartheta_s$  is integral with the global coordinates system. Once the source of the field problem is modeled, the procedure described in [15] can be followed to obtain the field solution due to permanent magnets in the airgap and winding regions. The radial component can be expressed as:

$$B_{wr,m}(r, \vartheta) = \sum_{n=1p,3p,\dots}^{\infty} K_B(n) f_{Br}(r, n) \cos(n\vartheta_r) \quad (14)$$

where the functions  $K_B(n)$  and  $f_{Br}(r, n)$  are written in the following for the inrunner case:

$$K_B(n) = \frac{(A_{zn}^m - nA_{zn}^m + \mu_0 M_{\vartheta n}) - 2\left(\frac{R_r}{R_m}\right)^{n+1} (A_{zn}^m + \mu_0 M_{\vartheta n}) + \left(\frac{R_r}{R_m}\right)^{2n} (A_{zn}^m + nA_{zn}^m + \mu_0 M_{\vartheta n})}{(\mu_r + 1) \left[ \left(\frac{R_r}{R_s}\right)^{2n} - 1 \right] + (\mu_r - 1) \left[ \left(\frac{R_m}{R_s}\right)^{2n} - \left(\frac{R_r}{R_m}\right)^{2n} \right]} \quad (15)$$

with  $A_{zn}^m$  defined as:

$$A_{zn}^m = \frac{\mu_0 (M_{\vartheta n} + nM_{rn})}{(n^2 - 1)} \quad (16)$$

$$f_{Br}(r, n) = \left(\frac{r}{R_s}\right)^{n-1} \left(\frac{R_m}{R_s}\right)^{n+1} + \left(\frac{R_m}{r}\right)^{n+1} \quad (17)$$

$$f_{B\vartheta}(r, n) = -\left(\frac{r}{R_s}\right)^{n-1} \left(\frac{R_m}{R_s}\right)^{n+1} + \left(\frac{R_m}{r}\right)^{n+1} \quad (18)$$

in particular,  $K_B(n)$  holds for any magnets pattern, as long as  $M_{rn}$  and  $M_{\vartheta n}$  in the expression are considering the contribution of all the magnets belonging to the array. It must be noticed that the case  $n = 1$ , i.e., the fundamental component of a two poles machine, must be treated separately. However, as the aim of the work is not to present an analytical model which could be applied for any type of machine topology. The aforementioned case, along with the outrunner case, is not considered and hence, not treated in the following. It is worthwhile pointing out that the generalized model, considering the latter two cases, has been developed by the authors and is fully applicable to the methodology described in the following section. The magnetic potential in the stator core is still governed by the Laplace's equation (1), and the solution keeps the same structure as the one shown in (2) but now only considering the harmonic components introduced by the magnets' field:

$$A_{z,m}(r, \theta) = \sum_{n=1p,3p,\dots}^{\infty} (G_n^+ r^n + G_n^- r^{-n}) \sin(n\theta_r) \quad (19)$$

The same boundary conditions as (5) and (6) can now be applied to the magnets field solution as it follows:

$$B_{r,m}^{st} \Big|_{r=R_{se}} = \frac{1}{r} \frac{\partial A_{z,m}}{\partial \vartheta_s} \Big|_{r=R_{se}} = 0 \quad (20)$$

$$\left( B_{r,m}^{st} = \frac{1}{r} \frac{\partial A_{z,m}}{\partial \vartheta_s} = B_{wr,m} \right) \Big|_{r=R_s} \quad (21)$$

giving again a linear system of two equations in the two variables  $G_n^+$  and  $G_n^-$ , whose solution yields to the following expressions:

$$G_n^+ = \frac{2R_s^n R_m \left(\frac{R_m}{R_s}\right)^n K_B(n)}{n(R_s^{2n} - R_{so}^{2n})} \quad (22)$$

$$G_n^- = -\frac{2R_{so}^{2n} R_s^n R_m \left(\frac{R_m}{R_s}\right)^n K_B(n)}{n(R_s^{2n} - R_{so}^{2n})}$$

By plugging (19) into (3) and (4), the resulting radial and circumferential components of the flux density in the stator core due to only the permanent magnets can be written as it follows:

$$B_{r,m}^{st}(r, \vartheta) = \sum_{n=1p,3p,\dots}^{\infty} G_S(n) f_{Sr}(r, n) \cos(n\vartheta_r) \quad (23)$$

$$B_{\vartheta,m}^{st}(r, \vartheta) = -\sum_{n=1p,3p,\dots}^{\infty} G_S(n) f_{S\vartheta}(r, n) \sin(n\vartheta_r) \quad (24)$$

The structure of the latter two flux density expressions follows the one adopted in [15] which appears to be optimized for numerical implementation. The functions  $G_S(n)$ ,  $f_{Sr}(r, n)$  and  $f_{S\vartheta}(r, n)$  are reported in the following:

$$G_S(n) = \frac{2K_B(n)}{\left[ \left(\frac{R_s}{R_{so}}\right)^{2n} - 1 \right]}$$

$$f_{Sr}(r, n) = \left(\frac{r}{R_{so}}\right)^{n-1} \left(\frac{R_m}{R_{so}}\right)^{n+1} - \left(\frac{R_m}{r}\right)^{n+1} \quad (25)$$

$$f_{S\vartheta}(r, n) = \left(\frac{r}{R_{so}}\right)^{n-1} \left(\frac{R_m}{R_{so}}\right)^{n+1} + \left(\frac{R_m}{r}\right)^{n+1}$$

### C. Validation of the Field Solution Against FE Analysis

The following part of the work takes a single case-study as a reference for the proposed methodology. Nevertheless, the procedure in itself holds for any machine, i.e., the analytical solution can be extended to other slotless topologies. The case-study is an inrunner six-pole machine mounting a 2-segment Halbach array (according to the notation adopted in [14]).

TABLE I  
SPM MACHINE DATA (COURTESY OF ALVA INDUSTRIES)

Parameter	Machine specification
$R_r$	27.6 mm
$R_m$	35.6 mm
$R_w$	37 mm
$R_s$	40 mm
$R_{so}$	48 mm
$B_r$	1.35 T
$\mu_{mag}$	1
$R_{mp}$	0.5
$p$	3
$I_n$	20 [Arms]

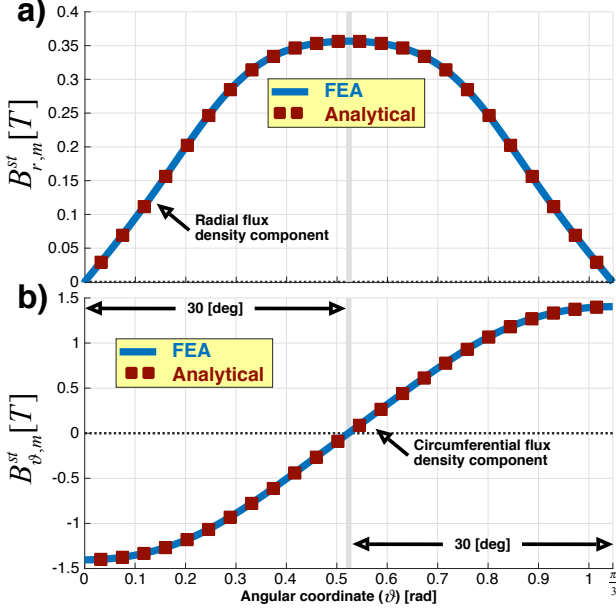


Fig. 2. Comparison between FEA and analytical solution of the flux density components due to PM in the middle of the stator core. a) Radial flux density,  $B_{r,m}^{st}$ . b) Circumferential flux density,  $B_{\theta,m}^{st}$ .

The analytical field solution, as obtained in the previous subsections, is here benchmarked against FE analysis of the same case-study described in I.

As shown in Fig. 2, the magnets field contribution finds a perfect correspondence between FEA and the analytical solution as written in eqs. (23) and (24). The latter validation considers a point placed in the middle of the stator core for the analytical solution and an arc at the same radius for the FE solution.

The same comparison is shown in Fig. 3 for the field contribution due to the stator currents. It can be noticed at a glance, that the field contribution due to the sinusoidal stator currents may not have a relevant impact in the iron losses; nevertheless, the latter observation will be proved, and criticized in the following loss analysis.

#### IV. ANALYTICAL-BASED IRON LOSS ESTIMATION

In the following, different iron loss models, taken from the literature, are briefly introduced and adopted with the proposed

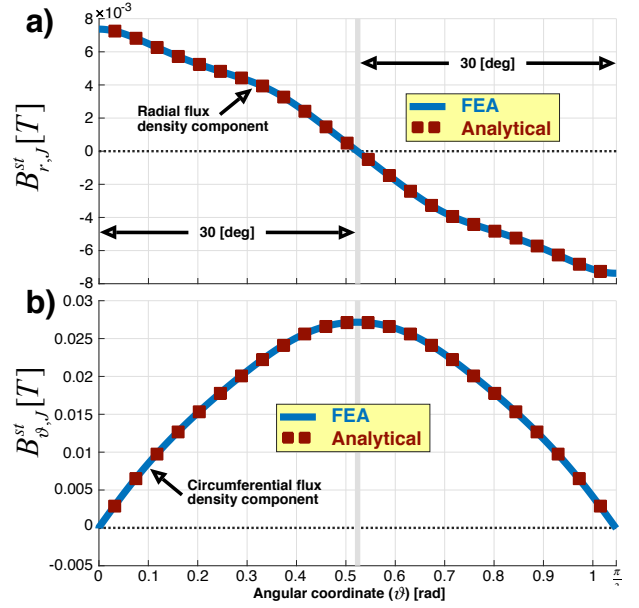


Fig. 3. Comparison between FEA and analytical solution of the flux density components due to stator current in the middle of the stator core (at  $t = 0$ ). a) Radial flux density,  $B_{r,J}^{st}$ . b) Circumferential flux density,  $B_{\theta,J}^{st}$ .

methodology to test its flexibility. The developed method will be presented as a post-processing procedure from the field solution as obtained in the previous section, to estimate iron losses in the laminated stator core.

#### A. Power Loss Models for Lamination Steel

In the iron losses evaluation for electric steel laminations, Bertotti's equations represent the most adopted and widely accepted model for estimating iron losses. In the frequency domain, the different specific loss contributions can be summed up in the following equation:

$$p = \underbrace{K_e B^2 f^2}_{P_e} + \underbrace{K_a B^{1.5} f^{1.5}}_{P_a} + \underbrace{K_h B^\alpha f}_{P_h} \quad (26)$$

where the three terms represent the eddy currents contribution, the hysteresis contribution, and the anomalous loss contribution, respectively. The different coefficients ( $K_e$ ,  $K_h$ ,  $K_a$ , and  $\alpha$ ) are to be determined by properly fitting the available experimental data.

When dealing with FEA element-based iron loss analysis, the following time-based analytical formulations becomes handier with the typical transient analysis [12], [13], [18], [19]:

$$p = \underbrace{\frac{K_e}{2\pi^2 T} \int_0^T \left| \frac{dB}{dt} \right|^2 dt}_{P_e} + \underbrace{\frac{K_a}{8.76 T} \int_0^T \left| \frac{dB}{dt} \right|^{1.5} dt}_{P_a} + \underbrace{\frac{K_h}{T} B^\alpha}_{P_h} \quad (27)$$

Different versions of the above-written equations have also been used. In [9], it was pointed out that the separation between eddy currents and anomalous loss contribution is questionable. Nevertheless, it is perceived that the adoption

of a good fitting model based on only hysteresis and eddy currents contributions would inevitably include anomalous loss phenomena, if any exists.

The adoption of constant loss coefficients may give reasonable results when the fitting to experimental data is optimized around the most probable, or rated operating condition. Thus, it can be a reasonable model when fixed speed operation and low load variation are expected. The physical phenomena governing iron losses in electrical steel laminations still represents a wide-open research topic for its inherent complexity. In fact, it is hard to imagine that a set of constant coefficients, adopted with any of the two above mentioned models, could extensively and accurately describe such phenomena in a wide frequency and flux density range.

In [8], [10], [11], different loss models based on variable loss coefficients ( $K_h(f, B)$  and  $K_e(f, B)$ ) are proposed, showing an improved fitting to experimental data compared to standard models based on constant coefficients. Referring to the models proposed in [9] and [10], two variable-coefficients-based iron loss models and a constant-coefficients-based model are developed and applied to the proposed analytical method. The results are finally compared.

### B. Rotational Loss Contribution

Another important aspect which is usually overlooked is the effect of having a rotational magnetic field when it comes to estimating iron losses. Although in some works, the assumption of having a purely alternating magnetic field is still considered [20]. It appears much more reasonable to accept the rotational nature of the flux density, whereby, in the iron region, the flux density variation is determined by the simultaneous pulsation of two orthogonal flux density components ([8], [19], [21]).

In Fig. 1 of [19], the variation of the two orthogonal flux density components is shown, for a slotted machine, in a tooth and in the back iron. The rotational behaviour of the field does not appear in the teeth. The latter may be one of the reasons why in some works the assumption of an alternating magnetic field may lead to reasonable results, as the loss contribution from the teeth may be the most relevant one ([22]). In this regard, considering slotless machines leads to the obvious conclusion that the rotational loss contribution has to be considered, being the flux density in the stator core rotational, by nature.

As for the rotational loss contribution, it appears to be widely accepted the rough procedure of summing up the alternating loss contribution from the two orthogonal components. However, it has been shown experimentally, in several instances [7], [23]–[25], that the latter methodology may lead to misleading iron loss estimate. Nonetheless, it is worth pointing out that characterizing the loss behaviour of a lamination specimen requires sophisticated pieces of equipment [24], [25] which are not generally available in any research lab.

An analytical extrapolation of the data presented in Fig. 3 of reference [23] will be used in the following to test the impact of the rotational effect.

### C. Stator Core Discretization Method for Iron Loss Analysis

As shown in the previous section, the field solution is known as a continuous function, in the whole 2-D domain, dependent on the radial and the angular position. Based on eqs. (26) or (27), the integration of the flux density function along the iron core surface is required for evaluating iron losses. As, in a general instance, the flux density is raised to a non-integer exponent, the analytical integration along the radial direction becomes not feasible; thus, a numerical integration based on the *rectangular rule* is proposed as an effective solution for the method. In the 2-D problem, the numerical integration consists in dividing the radial thickness of the iron core into smaller radial sub-segments whereon the flux density is assumed to be constant, namely, in each sub-segment, the flux density is only dependent on the rotor position. The latter operation is easily vectorizable and thus, computationally efficient.

Therefore, by using the loss model described in (26) the peak flux density ( $B$ ) becomes a matrix holding all the harmonic components in each radial sub-segment. Whereas, in eq. (27) the flux density is still a matrix containing the time-varying function (value in each time instant) on each sub-segment; thus, the differentiation can still be numerically approximated and vectorized. In particular, it comes fairly easy to apply this method to the load condition operation. In fact, the magnets field variation with the rotor angular coordinate represents the time variation with respect to the static coordinate ( $\vartheta_s$ ), while for the stator current field,  $\vartheta_s$  can be set equal to zero and the angle variation is given by  $\omega \cdot t$ . Moreover, the linearity of the problem does allow to add up the two different contributions in the iron core.

### D. Tested Iron Loss Models and Results

The different iron loss models are briefly described in the following without mentioning any quantity which may relate to the raw loss data for the secrecy of the data themselves, hoping that the provided information will be enough for applying the different models to any lamination loss data.

The loss analysis is carried out considering a rotational speed of 10000[*rpm*]; the full-load condition is considered in the first case. Where not explicitly specified, the losses are computed as the mere sum of iron losses due to radial and tangential components. The last case will consider the rotational effect for comparison.

1) *Constant Coefficients Model (CCM)*: The model uses equation (26) for fitting all the available lamination loss data to find a general equation to be applied to any frequency and flux density value. The comparison of the experimental loss data against the proposed fitting model produced a relative error which is shown in Fig. 4

Being the iron loss computation in time domain applied with the same algorithm both in FEA and to the analytical field solution, the results are expected to be the same (as shown in Table II). This being an indication of the losses to be expected, all the different frequency-based iron loss analyses are hereby applied only to the analytical model, considering only the no-load operating condition.

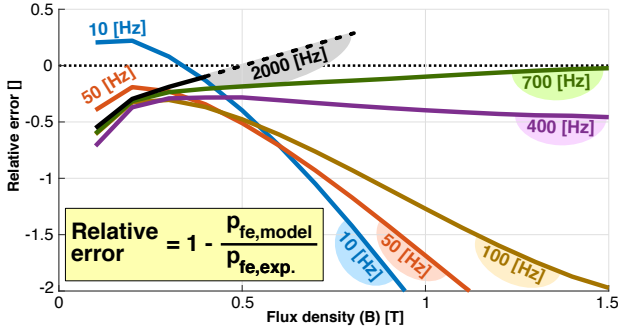


Fig. 4. Relative error between experimental loss data and estimated loss with (26) using constant coefficients (linear interpolation between available points)

TABLE II

FEA VALIDATION OF IRON LOSS WITH CONSTANT COEFFICIENTS MODEL

	Time Domain		Frequency Domain
	Full load	No load	No load
FEA	208.9 W	208.75 W	//
ANALYTICAL	208.8 W	208.73 W	212 W

2) *Two-Component Loss Model With Variable Coefficients (CAL2 [10])*: The power loss density function as reported in [10] is expressed as:

$$p = \underbrace{k_e(f, B)f^2 B^2}_{p_e} + \underbrace{k_h(f, B)f B^2}_{p_h} \quad (28)$$

where the dependency on the frequency of the coefficients  $k_h$  and  $k_e$  is neglected by splitting the experimental data into two frequency ranges where the only dependency on the flux density is considered. In particular, the first range considers all the loss curves in the range (10–100) Hz and a fifth-order polynomial is used to express the flux density dependency of the two coefficients, while in the second range (100–2000) Hz a third-order polynomial was shown to be enough for giving a good fit to the data.

A first comparison between Fig. 4 and Fig. 5 shows that this type of model can be extensively used in the whole experimental data range, without any need of re-fitting the experimental data themselves when a different operating point

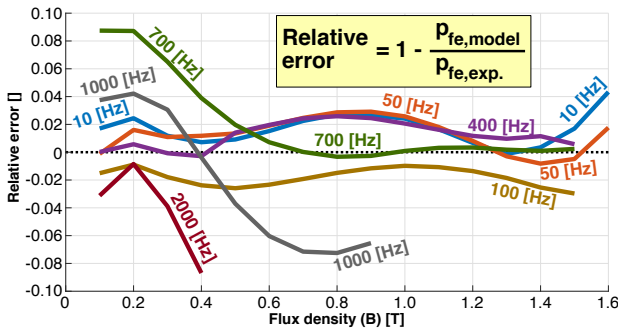


Fig. 5. Relative error between experimental loss data and estimated loss with CAL2 (10) iron loss model (linear interpolation between available points)

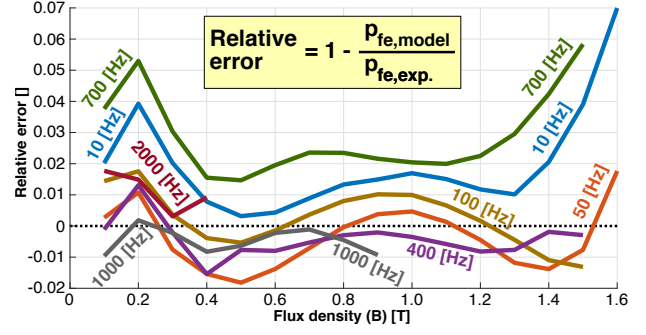


Fig. 6. Relative error between experimental data and estimated loss with all variable coefficients VARCOext (28) (interpolation between available points)

( $f, B$ ) is to be considered for the loss computation.

3) *Iron Loss Model With all Variable Coefficients (VARCOext)*: This model assumes the three components loss equation having all the coefficients as variable with flux density and frequency, and it can be seen as an extension of what is called VARCO in [10]:

$$p = \underbrace{k_e(f, B)f^2 B^2}_{p_e} + \underbrace{k_a(f, B)f^{1.5} B^{1.5}}_{p_a} + \underbrace{k_h(f, B)f B^{\alpha(f, B)}}_{p_h} \quad (29)$$

The method for finding the different coefficients follows extensively the procedure described in [9]; however, as the aim is to have an equation with explicit dependency on the frequency and flux density, the proposed representation of  $\alpha(f, B)$  and  $k_h(f, B)$ , which was based on some look-up tables in [9], was here approximated by means of interpolating functions giving a reasonable fit in the two different frequency ranges, which in this case were (10–400) Hz and (400–2000) Hz. The relative error with respect to the experimental data produced by this loss model is represented in Fig. 6.

4) *Rotational Field Effect Applied to VARCOext Loss Model (VARCOrot)*: With the aim of including the rotational effect in the iron loss computation model, VARCOext was chosen as a best-fit model for the iron losses calculation. The rotational loss factor function ( $\gamma$ ), can be expressed as:

$$\gamma = \frac{P_{rot}}{P(B_{maj}) + P(aB_{maj})} \quad (30)$$

where  $a$  is the ratio between minor axis ( $B_{min}$ ) and major axis ( $B_{maj}$ ) component in the iron core flux density locus. From the analytical field solution, it is easy to extract major and minor axis components; therefore, the axis ratio can be found over each radial sub-segment for each harmonic component. Meaning that, yet again, an analytical function  $\gamma(a, B_{maj})$  can be easily applied to the iron loss estimation method as a correction for the results obtained with the previous models based on summing the contribution of the two orthogonal components. The experimental results presented in Fig. 3 of reference [23] were conveniently extrapolated. However, it is worth mentioning that the experimental data in the same reference were obtained at 50 Hz fixed frequency, meaning that, being the fundamental frequency of the proposed

operating point equal to 500 Hz, the correction function itself may lead to misleading results for this very case.

TABLE III

COMPARISON OF FREQUENCY-BASED IRON LOSS MODELS (NO-LOAD)

	CCM	CAL2	VARCOext	VARCORot
Total Iron Losses	212 W	169.81 W	163.42 W	155.75 W
Deviation	+36.11 %	+9.03 %	+4.92 %	0 %

In Table III, the results obtained with the four different models are compared. While the difference between CCM, CAL2 and VARCOext can be deduced by the different figures showing the relative error produced by each model (Fig. 4,5,6), the loss reduction with the rotational effect included (VARCORot) can be explained by looking at Fig. 3 in reference [23]. In fact, in the proposed case study, the main losses are due to a fundamental flux density which is greater than 1 [T], with an axis ratio having a maximum value of about 0.5 in the proximity of the stator winding. This means that the loss factor  $\gamma$  acts as a reduction factor for the iron losses computed as a mere sum of the two orthogonal contributions.

## V. CONCLUSION

In this paper, the analytical field solution in the stator iron core of slotless machines is derived from Maxwell's equations. The field results were bench-marked against FEA to verify their accuracy. The proposed method for post-processing the field results and calculate the iron losses, is described. The flexibility of the method was tested by using different iron loss models, suggesting that the problem can be easily vectorized, thus, leading to a computationally efficient procedure which could be used already in a pre-design phase and/or optimization procedure. The different loss models showed that having a good fit to experimental loss data of a given specimen maybe even more important than having a very accurate field solution for evaluating iron losses. In this regard, some best-fit iron loss models were proposed to overcome the latter issue. Finally, the model has been assessed to give good correspondence with FEA analysis using non-linear iron material under the saturation region (typical design for slotless SPMs).

## REFERENCES

- [1] A. Tassarolo, L. Branz, and C. Bruzzese, "A compact analytical expression for the load torque in surface permanent-magnet machines with slotless stator design," in *Proc. IEEE Work. Elect. Mach. Design. Contr. Diag.*, March 2013, pp. 8–17.
- [2] N. Bianchi, S. Bolognani, and F. Luise, "Analysis and design of a pm brushless motor for high-speed operations," *IEEE Trans. Energy Convers.*, vol. 20, no. 3, pp. 629–637, Sep. 2005.
- [3] A. Chebak, P. Viarouge, and J. Cros, "Analytical model for design of high-speed slotless brushless machines with smc stators," in *Proc. IEEE Int. Elect. Mach. Drives Conf.*, vol. 1, May 2007, pp. 159–164.
- [4] A. Tassarolo, M. Bortolozzi, and C. Bruzzese, "Explicit torque and back emf expressions for slotless surface permanent magnet machines with different magnetization patterns," *IEEE Trans. Magn.*, vol. 52, no. 8, pp. 1–15, Aug 2016.
- [5] A. Rahideh, M. Mardaneh, and T. Korakianitis, "Analytical 2-d calculations of torque, inductance, and back-emf for brushless slotless machines with surface inset magnets," *IEEE Trans. Magn.*, vol. 49, no. 8, pp. 4873–4884, Aug 2013.
- [6] L. Branz, M. Bortolozzi, and A. Tassarolo, "Analytical calculation of the no-load flux density in the stator core of slotless spm machines," in *Proc. Int. Conf. Workshop Compatib. Power Electron.*, June 2013, pp. 244–249.
- [7] C. A. Hernandez-Aramburo, T. C. Green, and A. C. Smith, "Estimating rotational iron losses in an induction machine," *IEEE Trans. Magn.*, vol. 39, no. 6, pp. 3527–3533, Nov 2003.
- [8] J. Seo, T. Chung, C. Lee, S. Jung, and H. Jung, "Harmonic iron loss analysis of electrical machines for high-speed operation considering driving condition," *IEEE Trans. Magn.*, vol. 45, no. 10, pp. 4656–4659, Oct 2009.
- [9] D. M. Ionel, M. Popescu, S. J. Dellinger, T. J. E. Miller, R. J. Heideman, and M. I. McGilp, "On the variation with flux and frequency of the core loss coefficients in electrical machines," *IEEE Trans. Ind. Appl.*, vol. 42, no. 3, pp. 658–667, May 2006.
- [10] D. M. Ionel, M. Popescu, M. I. McGilp, T. J. E. Miller, S. J. Dellinger, and R. J. Heideman, "Computation of core losses in electrical machines using improved models for laminated steel," *IEEE Trans. Ind. Appl.*, vol. 43, no. 6, pp. 1554–1564, Nov 2007.
- [11] M. Popescu and D. M. Ionel, "A best-fit model of power losses in cold rolled-motor lamination steel operating in a wide range of frequency and magnetization," *IEEE Trans. Magn.*, vol. 43, no. 4, pp. 1753–1756, April 2007.
- [12] M. Desvaux, B. Multon, S. Sire, and H. Ben Ahmed, "Analytical iron loss model for the optimization of magnetic gear," in *Proc. Int. Elect. Mach. Drives Conf.*, May 2017, pp. 1–8.
- [13] Z. Djelloul-Khedda, K. Boughrara, F. Dubas, A. Kechroud, and A. Tikel-laline, "Analytical prediction of iron-core losses in flux-modulated permanent-magnet synchronous machines," *IEEE Trans. Magn.*, vol. 55, no. 1, pp. 1–12, Jan 2019.
- [14] Y. Shen and Z. Zhu, "General analytical model for calculating electro-magnetic performance of permanent magnet brushless machines having segmented halbach array," *IET Elect. Syst. Transport.*, vol. 3, no. 3, pp. 57–66, Sep. 2013.
- [15] Z. Q. Zhu, D. Howe, and C. C. Chan, "Improved analytical model for predicting the magnetic field distribution in brushless permanent-magnet machines," *IEEE Trans. Magn.*, vol. 38, no. 1, pp. 229–238, Jan 2002.
- [16] Y. Shen and Z. Q. Zhu, "Investigation of permanent magnet brushless machines having unequal-magnet height pole," *IEEE Trans. Magn.*, vol. 48, no. 12, pp. 4815–4830, Dec 2012.
- [17] —, "Analysis of electromagnetic performance of halbach pm brushless machines having mixed grade and unequal height of magnets," *IEEE Trans. Magn.*, vol. 49, no. 4, pp. 1461–1469, April 2013.
- [18] M. A. Mueller, S. Williamson, T. J. Flack, K. Atallah, B. Baholo, D. Howe, and P. H. Mellor, "Calculation of iron losses from time-stepped finite-element models of cage induction machines," in *Proc. IEEE Int. Conf. Elect. Mach. Drives*, Sep. 1995, pp. 88–.
- [19] P. A. Hargreaves, B. C. Mecrow, and R. Hall, "Calculation of iron loss in electrical generators using finite element analysis," in *Proc. IEEE Int. Elect. Mach. Drives Conf.*, May 2011, pp. 1368–1373.
- [20] C. A. Hernandez-Aramburo, T. C. Green, and A. C. Smith, "Assessment of power losses of an inverter-driven induction machine with its experimental validation," in *Proc. IEEE Ind. Appl. Conf. 37th IAS Ann. Meet.*, vol. 2, Oct 2002, pp. 1127–1134 vol.2.
- [21] Lei Ma, M. Sanada, S. Morimoto, and Y. Takeda, "Prediction of iron loss in rotating machines with rotational loss included," *IEEE Trans. Magn.*, vol. 39, no. 4, pp. 2036–2041, July 2003.
- [22] K. Komezda and M. Dams, "Finite-element and analytical calculations of no-load core losses in energy-saving induction motors," *IEEE Trans. Ind. Electron.*, vol. 59, no. 7, pp. 2934–2946, July 2012.
- [23] T. Kochmann, "Relationship between rotational and alternating losses in electrical steel sheets," *J. Magn. Magnet. Mater.*, vol. 160, pp. 145–146, 1996.
- [24] M. Enokizono, T. Suzuki, J. Sievert, and J. Xu, "Rotational power loss of silicon steel sheet," *IEEE Trans. Magn.*, vol. 26, no. 5, pp. 2562–2564, Sep. 1990.
- [25] N. Stranges and R. D. Findlay, "Measurement of rotational iron losses in electrical sheet," *IEEE Trans. Magn.*, vol. 36, no. 5, pp. 3457–3459, Sep. 2000.